Inorganic Chemistry

Article

pubs.acs.org/IC

Tetrapalladium-Containing Polyoxotungstate $[Pd^{II}_4(\alpha\text{-}P_2W_{15}O_{56})_2]^{16-}$: A Comparative Study

Natalya V. Izarova,[†,⊥] Raisa I. Maksimovskaya,[§] Sabine Willbold,[‡] and Paul Kögerler*[,†,∥]

[†]Peter Grünberg Institute—PGI 6 and [‡]Central Institute for Engineering, Electronics and Analytics—ZEA-3, Forschungszentrum Jülich, D-52425 Jülich, Germany

[§]Boreskov Institute of Catalysis, 630090 Novosibirsk, Russia

[∥]Institute of Inorganic Chemistry, RWTH Aachen University, D-52074 Aachen, Germany

Supporting Information

ABSTRACT: The novel tetrapalladium(II)-containing polyoxometalate $[Pd^{II}_4(\alpha\text{-}P_2W_{15}O_{56})_2]^{16-}$ has been prepared in aqueous medium and characterized as its hydrated sodium salt $Na_{16}[Pd_4(\alpha\text{-}P_2W_{15}O_{56})_2]\cdot 71H_2O$ by single-crystal XRD, elemental analysis, IR, Raman, multinuclear NMR, and UV−vis spectroscopy. The complex exists in anti and syn conformations, which form in a 2:1 ratio, and possesses unique structural characteristics in comparison with known $\{M_4(P_2W_{15})_2\}$ species. ^{31}P and ^{183}W NMR spectroscopy are consistent with the long-term stability of the both isomers in aqueous solutions.

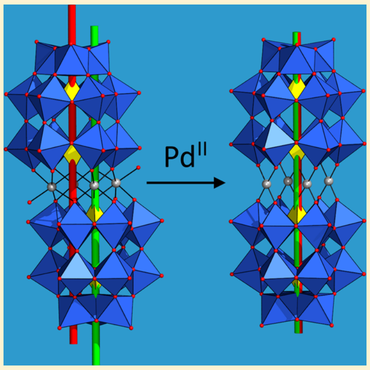

INTRODUCTION

Pd^{II} complexes with polyoxotungstates (POTs) have attracted considerable attention during the last years as potential catalysts or precatalysts for various low-temperature transformations of organic substrates.[1,2] On the other hand, the square-planar Pd^{II} coordination environment [in contrast to octahedral coordination characteristic for the first-row transition metals, the reactivity of which toward polyoxometalates (POMs) is widely investigated] opens possibilities to design polyanions with unique, so far not observed, structures and properties. In this context, a novel class of polyanions based exclusively on Pd^{II} and Au^{III} centers has been discovered in the past decade,[2b,3] and very recently, several unusual seleno- and tellurotungstates incorporating multinuclear Pd^{II}-based fragments reminiscent of building blocks that constitute polyoxopalladate structures have been reported.[4]

Nevertheless, the number of structurally characterized Pd-containing polyanions remains quite small in comparison with that of POMs incorporating 3d metals and lanthanides, and the other examples include only a few Pd^{II} complexes with lacunary POTs[5−9] as well as 1D polymers where Pd^{II} ions link paratungstate species into infinite chains.[10] In this respect it was shown that monolacunary Lindqvist-, Keggin-, and Wells−Dawson-type POTs form polyanions $[Pd^{II}_2(W_5O_{18})_2]^{8-}$, $[Pd^{II}_2(\alpha\text{-}PW_{11}O_{39})_2]^{10-}$, and *syn*/*anti*-$[Pd^{II}_2(\alpha_2\text{-}P_2W_{17}O_{61})_2]^{16-}$, respectively, where two Pd^{II} ions in a square-planar environment link together the two POM ligands.[5] When the dilacunary derivatives of Keggin-type silicotungstate are reacted with Pd^{II} acetate, they form monomeric $[\gamma\text{-}H_2SiW_{10}O_{36}Pd_2(CH_3COO)_2]^{4-}$ species where two Pd^{II} centers grafted on the vacant site of the POT are additionally bridged by two acetates.[1m] Interaction of this complex with dicarboxylates led to carboxylate metathesis and formation of dimeric assemblies of the constitution $[\{(\gamma\text{-}H_2SiW_{10}O_{36}Pd_2)\text{-}(O_2C(CH_2)_nCO_2)\}_2]^{8-}$ (n = 1, 3, 5).[6] A number of sandwich-like complexes with general formulas $[Pd_{3-y}(WO_2)_y(XW_9O_{34})_2]^{z-}$ (X = P^V, Si^{IV})[7] and $[Pd_{3-y}(WO_2)_y(XW_9O_{33})_2]^{z-}$ (X = As^{III}, Sb^{III}, Te^{IV})[8] are built by two trilacunary Keggin-type $\{XW_9\}$ units linked either via three Pd^{II} centers (y = 0) or via a belt comprising one Pd^{II} and two WO_2 groups (y = 2) or two Pd^{II} centers and one WO_2 group (y = 1), depending on the exact reaction conditions. Interaction of Pd^{II} with trilacunary bismuthotungstate $[BiW_9O_{33}]^{9-}$ resulted in the Krebs-type structure $[Pd_3(H_2O)_9Bi_2W_{22}O_{76}]^{8-}$, where Pd^{II} ions are only weakly bound to the POT surface.[9]

At the same time, almost no attention has been given to the reactivity of Pd^{II} toward lacunary derivatives of Wells−Dawson-type POMs, and the above-mentioned syn and anti isomers of $[Pd^{II}_2(\alpha_2\text{-}P_2W_{17}O_{61})_2]^{16-}$ are the only known structurally characterized Pd^{II} complexes with POTs of this structural type. Herein we report the novel sandwich-like polyanion $[Pd_4(\alpha\text{-}P_2W_{15}O_{56})_2]^{16-}$ (**1**) exhibiting unique structural features, which was obtained in the reactions of Pd^{II} ions with the trilacunary Wells−Dawson-type POT [α-

Received: August 28, 2014
Published: October 17, 2014

$P_2W_{15}O_{56}]^{12-}$ and isolated as the hydrated sodium salt $Na_{16}[Pd_4(\alpha\text{-}P_2W_{15}O_{56})_2]\cdot 71H_2O$ (**Na-1**) and the tetrabutylammonium salt $[(C_4H_9)_4N]_{15}[HPd_4(\alpha\text{-}P_2W_{15}O_{56})_2]$ (**TBA-1**).

■ RESULTS AND DISCUSSION

Synthesis. The polyanion **1** self-assembles in the reaction of Pd^{II} nitrate and $[\alpha\text{-}P_2W_{15}O_{56}]^{12-}$ in 0.5 M CH_3COONa medium in the pH range of 2−8 and the temperature range of 5−80 °C. Variation of the Pd^{II}:P_2W_{15} ratio from 3:1 to 1:1 also does not influence the composition of the final product, which is crystallized from the $Pd^{II}/\{P_2W_{15}\}/0.5$ M CH_3COONa reaction systems, and **Na-1** has been isolated in all the cases as based on ^{31}P NMR and IR spectroscopy as well as unit cell measurements. **Na-1** is well-soluble in water (>0.25 g/1 mL) at room temperature, is also soluble in 1:1 mixtures of $H_2O/(CH_3)_2CO$ and H_2O/CH_3CN, and can be repeatedly recrystallized from water and 0.5 M CH_3COONa (pH 4.2).

The tetrabutylammonium salt, **TBA-1**, soluble in common organic solvents (e.g. CH_3CN, $(CH_3)_2CO$, CH_2Cl_2), was prepared by dropwise addition of an aqueous solution of **Na-1** to an aqueous solution of $TBAHSO_4$, followed by washing of the obtained precipitate with plenty of water, and its identity and purity were confirmed using IR, ^{31}P NMR, and C, H, N analysis.

Crystal Structure Analysis. Compound **Na-1** crystallizes in the triclinic symmetry in the space group $P\bar{1}$. The polyanions **1** possess a sandwich-like structure where two phosphotungstate units $[\alpha\text{-}P_2W_{15}O_{56}]^{12-}$ (=$\{P_2W_{15}\}$) are linked via a belt of four Pd^{II} centers (Figure 1).

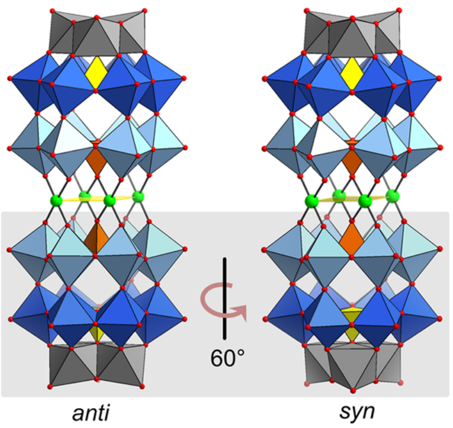

Figure 1. Structure of the *anti*-**1** (left) and *syn*-**1** (right) polyanions. WO_6 octahedra: W_3O_6 cap, gray; inner W_6O_{27} belts, dark blue; outer W_6O_{27} belts, light blue. P^AO_4 and P^BO_4, yellow and orange tetrahedra, respectively; Pd, green spheres; O, red. The Pd_4 plane is emphasized as a transparent yellow rhombus. Rotation of the lower $\{P_2W_{15}\}$ group by 60° transforms the isomers into each other.

There is a complex disorder of $[Pd_4(\alpha\text{-}P_2W_{15}O_{56})_2]^{16-}$ polyanions in the crystals of **Na-1**, implying (1) a rotation of $\{P_2W_{15}\}$ ligands by 60°, which results in two symmetrically independent positions of $\{P_2W_{15}\}$ with the relative occupancies of 66 and 34%, respectively, and (2) a rotation of the Pd_4 belt by +60° and −60°, resulting in three symmetrically independent positions for the Pd_4 rhomb with the relative occupancies of 66% (nonrotated), 23% (rotated to +60°), and 11% (rotated to −60°). Such kind of disorder implies, on the one hand, that part of the polyanions $[Pd_4(\alpha\text{-}P_2W_{15}O_{56})_2]^{16-}$ can be turned relative to each other by either +60° or −60° during their packing in the crystals of **Na-1**. One the other hand, such a hypothesis does not explain the nonequal distribution of the "rotated" and "nonrotated" positions for **1**, which is exactly reproducible from crystal to crystal. Another explanation is the turn of only one of the $\{P_2W_{15}\}$ ligands in part of polyanions **1** relative to the remaining $\{Pd_4P_2W_{15}\}$ unit by 60°, which results in syn/anti isomerism, with an *anti*-**1** to *syn*-**1** isomer ratio of 2:1, respectively (66% vs 34%). It should be noted that the rotation of $\{P_2W_{15}\}$ vs $\{Pd_4P_2W_{15}\}$ by either +60° or −60° would equally lead to the syn derivative. The second scenario and the presence of both anti and syn isomers in this exact ratio have been confirmed by ^{31}P and ^{183}W NMR spectroscopy (vide infra).

The $\{P_2W_{15}\}$ ligands in **1** have a typical Wells−Dawson structure, with one W_3O_6 "capping" group missing, and consist of two central tetrahedral PO_4 templates surrounded by 15 corner- and edge-shared WO_6 octahedra (Figure 1). The polyanions possess C_{3v} symmetry with the C_3 axis passing through the two P^V ions. The 15 WO_6 octahedra can be formally divided into a W_3O_6 "cap" (gray in Figure 1) and an "inner" W_6O_{27} "belt" (dark blue) assembled around the P^AO_4 units (yellow tetrahedra) and an "outer" W_6O_{27} "belt" (light blue) placed around the second P^BO_4 group (orange). Due to the missing second W_3O_6 cap, the phosphotungstate $\{P_2W_{15}\}$ offers a so-called vacant or lacunary site with seven nucleophilic oxygen atoms suitable for coordination to various heterometals. Six of these oxygens coordinated to six W^{VI} centers of the outer W_6O_{27} belt form a nearly regular hexagon ($O\cdots O_{average}$ = 3.08 Å), which is centered by an oxygen of the PO_4 group (Supporting Information, Figure S1, left). The W−O and P−O bond lengths in **1** are in the usual range.

All four Pd^{II} ions in the complex with $\{P_2W_{15}\}$ exhibit square-planar coordination. Two of them, situated on the opposite side of the Pd_4 rectangle, coordinate an oxygen atom of one of the WO_6 units [Pd−O = 1.985(15)−2.096(10) Å] and an oxygen atom of the P^BO_4 group [Pd−O = 2.029(15)−2.057(18) Å]. With respect to the geometry of the vacant site of $\{P_2W_{15}\}$, the two Pd^{II} ions of this structural type bind the two opposite oxygen atoms of the O_6 hexagon and the central O atom, which they share between each other [$Pd\cdots Pd$ = 3.121(4) Å]. The type of coordination of these two Pd^{II} ions is the same for the both anti and syn isomers of **1**.

Each of the other two Pd^{II} ions in the anti isomer of **1** coordinates two oxygens of the edge-shared W_2O_{10} unit of one POM ligand and two oxygens of the corner-shared W_2O_{11} unit of the second $\{P_2W_{15}\}$ species [Pd−O = 1.978(15)−2.215(18) Å]. Thus, the *anti*-**1** polyanions are centrosymmetric and belong to C_{2h} point symmetry group (Figure 1, left). In terms of the geometry of the vacant site of every $\{P_2W_{15}\}$ ligand, these two Pd^{II} centers coordinate oxygens of two opposite sides of a centered $\{O_6\}$ hexagon, which remain noncoordinated by the Pd^{II} ions of the first structural type (Supporting Information, Figure S1, right). The $Pd\cdots Pd$ distance is 5.576(3)−5.621(3) Å for the palladium centers of this structural type and 3.182(9)−3.192(19) Å between the palladium(II) ions of the first and second structural types.

In the syn isomer the Pd^{II} centers of the second structural type are not equivalent: one of them binds oxygen atoms of the edge-shared W_2O_{10} unit of every $\{P_2W_{15}\}$ ligand, and the second one, correspondingly, coordinates oxygens of the corner-shared W_2O_{11} groups of each $\{P_2W_{15}\}$. Overall the syn derivative of **1** possesses idealized C_{2v} symmetry (Figure 1, right).

The 2:1 ratio between the anti and syn isomers of **1** does not change by reacting Pd^{II} and $\{P_2W_{15}\}$ at various pH values (from 2.0 to 7.8) or different temperatures (including reaction and crystallization of **Na-1** at 5 °C, as well as prolonged heating of the reaction mixture at 80 °C). It also remains unchanged by performing the reaction in other Na^+-containing media (e.g. 0.5 M Na_2SO_4 and $NaClO_4$ aqueous solutions), as based on ^{31}P NMR spectroscopy as well as the unit cell and, in some cases, complete crystal structure measurements. Importantly, ^{31}P NMR spectra of the reaction mixtures of Pd^{II} and $\{P_2W_{15}\}$ in CH_3COONa solutions showed that this ratio is not driven by crystal packing of the isomers in **Na-1** and appears already before crystallization (Supporting Information, Figure S6). It is also interesting to note that complex **1** does not form by reacting Pd^{II} and $\{P_2W_{15}\}$ in water based on the ^{31}P NMR spectra of the $Pd^{II}/\{P_2W_{15}\}/H_2O$ system.

The formation of the two isomers of $[Pd_4(\alpha\text{-}P_2W_{15}O_{56})_2]^{16-}$ is in agreement with the prior observation of syn and anti derivatives in Pd^{II} complexes with monolacunary Wells–Dawson phosphotungstates $\{\alpha_2\text{-}P_2W_{17}\}$.[5c] However, in that case the significantly different shape of the anti and syn isomers of $[Pd_2(\alpha_2\text{-}P_2W_{17}O_{61})_2]^{16-}$ resulted in the different solubility of their alkali metal salts and thus allowed isolations of both derivatives in the pure state. Unfortunately, the relatively high C_{3v} symmetry of $\{P_2W_{15}\}$ ligands and the very similar stereochemistry of *anti*-**1** and *syn*-**1** render their separation hardly feasible at the moment. However, we are trying to isolate other (Rb^+, Cs^+, or organic) salts of **1** with the aim of separating the isomers or changing their relative ratio.

It is also interesting to compare the structure of **1** with that of well-known $[M_4(H_2O)_2(P_2W_{15}O_{56})_2]^{n-}$ (=$\{M_4(P_2W_{15})_2\}$) complexes formed by octahedrally coordinated transition metal centers (M = Mn^{II}, Fe^{III}, Co^{II}, Ni^{II}, Cu^{II}, Zn^{II}, and Cd^{II}).[11] Like in **1**, the typical structure of a $\{M_4(P_2W_{15})_2\}$ complex comprises a tetrametal belt $M_4(H_2O)_2$ sandwiched between two $\{P_2W_{15}\}$ phosphotungstates. At the same time, the higher coordination number of 6 for the M^{m+} centers in $M_4(H_2O)_2$ (compared with CN = 4 for Pd^{II} in **1**) leads to significant structural differences. Thus, every O atom associated with the P^BO_4 group at the lacunary site of $\{P_2W_{15}\}$ in $\{M_4(P_2W_{15})_2\}$ is coordinated not by two ions as in **1** but by three M^{m+} ions at the same time. Two of the four M^{m+} centers in $M_4(H_2O)_2$ coordinate to P^BO_4 groups of both $\{P_2W_{15}\}$ ligands (which could be compared with the two Pd^{II} of the first structural type in **1**), whereas the remaining two M^{m+} ions only bind to a P^BO_4 of only one $\{P_2W_{15}\}$ ligand. This results in a parallel shift of the main axes of the $\{P_2W_{15}\}$ units in $\{M_4(P_2W_{15})_2\}$, while the C_3 axes of each $\{P_2W_{15}\}$ unit coincide and pass through the center of the Pd_4 rhombus (Supporting Information, Figure S2). From an alternative point of view, the three MO_6 octahedra in the $M_4(H_2O)_2$ belt coordinating to P^BO_4 form $\{M_3P_2W_{15}\}$ units akin to *β*-type Wells–Dawson structures, and the common $\{M_4(P_2W_{15})_2\}$ structure can be regarded as a centrosymmetrical *ββ*-isomer.[11] In the case of M = Co^{II}, it was shown that a mixture of *ββ*- and *αβ*-isomers (which differ from *ββ* by a 60° rotation of one of the $\{P_2W_{15}\}$ units with respect to the $\{M_4P_2W_{15}\}$ part) coexists in reaction mixtures at neutral pH values.[11i] This is in direct analogy with anti/syn isomerism in the $\{Pd_4(P_2W_{15})_2\}$ complex.

In summary, the Pd^{II}-based complex **1**, $\{Pd_4(P_2W_{15})_2\}$, in comparison to conventional $\{M_4(P_2W_{15})_2\}$-type structures, exhibits structural similarities, in particular, the similar rhombic arrangement of the four metal centers of the inner belt of the polyanions and the ability to form isomers that differ by 60° rotation of one of the $\{P_2W_{15}\}$ groups with respect to the $\{M_4P_2W_{15}\}$ unit. At the same time, **1** displays unique structural characteristics imparted by the square-planar coordination environment of Pd^{II} ions, implying that the local C_3 axes of the two $\{P_2W_{15}\}$ groups coincide and formation of the syn isomers also in acidic media.

The structure of **1** is also unique in comparison with structurally characterized sandwich-like Pd^{II} complexes of the trilacunary Keggin-type species $[A\text{-}\alpha\text{-}(XO_4)W_9O_{30}]^{n-}$ and $[B\text{-}\alpha\text{-}(XO_3)W_9O_{30}]^{n-}$ (=$\{XW_9\}$), $\{Pd_3(XW_9)_2\}$.[7,8] Compared to $\{XW_9\}$, the vacant site of $\{P_2W_{15}\}$ offers an additional central oxygen atom of the P^BO_4 group due to the different orientation of the XO_4 tetrahedron in the B-*α*- and A-*α*-trilacunary POT derivatives (Supporting Information, Figure S3). Also in $\{B\text{-}\alpha\text{-}XW_9\}$ this additional oxygen is absent and replaced by a lone pair on the central $X^{III/IV}$ heteroion (X = As^{III}, Sb^{III}, Te^{IV}). This feature allows for coordination of four Pd^{II} centers in **1** while the sandwich-like complexes of Pd^{II} with $\{XW_9\}$ POTs contain only up to three noble metal ions. On the other hand, the formation of $[Pd_4(B\text{-}\alpha\text{-}PW_9O_{34})_2]^{10-}$ polyanions based on UV–vis, photocolorimetry, and conductometry data was proposed.[11] $\{Pd_4(B\text{-}\alpha\text{-}PW_9)_2\}$ should possess a structure similar to **1**, where the $\{P_2W_{15}\}$ ligands are replaced by $[B\text{-}\alpha\text{-}PW_9O_{34}]^{9-}$ POTs. However, there still is no structural evidence for the formation of a complex with $\{Pd_4(B\text{-}\alpha\text{-}PW_9)_2\}$ stoichiometry, and our attempts to isolate such a derivative have so far failed, leading to the well-characterized[7a−c] $[Pd_3(A\text{-}\alpha\text{-}PW_9O_{34})_2]^{12-}$ species.

IR Spectroscopy. The IR spectrum of **Na-1** exhibits three absorption bands at 1090, 1065, and 1016 cm^{-1}, which could be assigned to vibrations of P–O bonds. They could be compared with the P–O vibrations bands at 1130, 1086, and 1009 cm^{-1} for $Na_{12}[\alpha\text{-}P_2W_{15}O_{56}]\cdot 24H_2O$ (Na-$\{P_2W_{15}\}$) (Supporting Information, Figure S4, and refs 11a and 12) and at 1090 and 1012 cm^{-1} for $K_6[\alpha\text{-}P_2W_{18}O_{62}]\cdot 14H_2O$ (Supporting Information, Figure S4, and refs 12 and 13). The disappearance of the band at 1130 cm^{-1} characteristic for noncoordinated $\{P_2W_{15}\}$ and the appearance a new band at 1065 cm^{-1} are in agreement with the coordination of one of the oxygen atoms of P^BO_4 group at the lacunary site of the $\{P_2W_{15}\}$ ligands by Pd^{II} in **1**. The band characteristic for terminal W═O bonds appears at 941 cm^{-1}. The set of bands in the range of 909−767 cm^{-1} could be assigned to vibrations of W–O–W and W–O–Pd bonds. The significant shift of these bands compared to the W–O–W bands in noncoordinated $\{P_2W_{15}\}$ (see the Supporting Information, Figure S4) is also consistent with formation of a coordination complex between Pd^{II} and $\{P_2W_{15}\}$ in **Na-1**. A band at 563 cm^{-1}, which is absent in the spectrum of Na-$\{P_2W_{15}\}$, corresponds to Pd–O valence bands.[14] The IR spectrum of **TBA-1** exhibits similar features and additional bands corresponding to C–C, C–N, and C–H vibrations of the TBA^+ countercations (Supporting Information, Figure S5)

NMR Spectroscopy. The room temperature ^{31}P NMR spectrum of **1** (Figure 2) exhibits three signals at −3.4, −3.6, and −14.6 ppm with the relative intensities of 2:1:3, which could be compared with the signals at +0.1 and −13.3 ppm for the noncoordinated $\{P_2W_{15}\}$ ligands[12] and the lines at −4.3 and −14.3 ppm for $\{Zn_4(P_2W_{15})_2\}$.[11b] The most intense signal at −14.6 ppm stems from the P^AO_4 group of the $\{P_2W_{15}\}$ ligands and it appears to be not sensitive to the anti/syn isomerization. The two downfield signals originate from the P^BO_4 close to the Pd_4 belt. On the basis of the relative

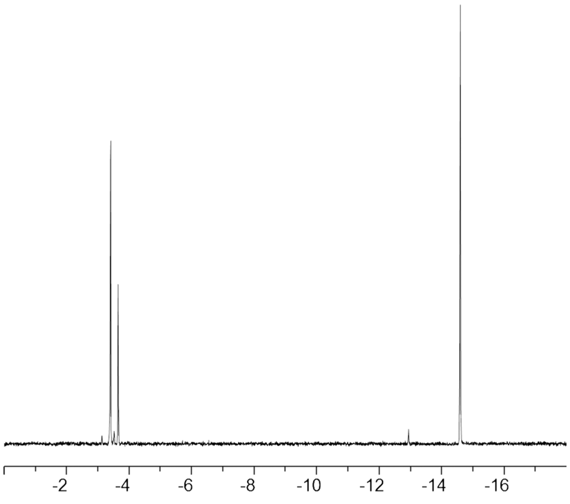

Figure 2. Room temperature ^{31}P NMR spectrum of **Na-1** redissolved in H_2O/D_2O (the three small signals belong to minor impurities that do not exceed 2%).

intensities of these two signals, which are in a very good agreement with the solid-state X-ray data, the signal at −3.4 ppm could be assigned to the *anti*-**1** isomer, while the signal at −3.6 ppm belongs to the *syn*-**1** derivative. Spectra measured at 278 K (Supporting Information, Figure S7) and 353 K (Supporting Information, Figure S8) both exhibit the same three signals, although their chemicals shifts differ slightly compared to those of the room temperature spectrum (−2.9, −3.1, and −14.1 ppm at 278 K and −4.0, −4.2, and −15.2 ppm at 353 K). The relative intensity of the two downfield signals in these spectra indicates the same 2:1 ratio between the anti and syn isomers of **1**, confirming the absence of dynamic phenomena associated with the complex dissociation and isomerization in aqueous medium at various temperatures.

The spectrum remains unchanged for a long period of time, indicating high solution stability of the polyanions **1** in aqueous medium.

The room temperature ^{183}W NMR spectrum of aqueous **Na-1** solution exhibits 15 signals (Figure 3), in good agreement with the expected pattern, based on the solid-state structure. The $\{P_2W_{15}\}$ ligands in both anti and syn isomers of **1** acquire local C_s symmetry with the vertical mirror plane intersecting the two Pd^{II} ions of the second structural type and one of the W^{VI} center of the W_3O_{13} cap. The mirror plane divides the W centers of each $\{P_2W_{15}\}$ unit into seven pairs of symmetry-equivalent atoms and the unique polar W site, similar to the patterns observed for the $\{M_4(P_2W_{15})_2\}$ series (M = Co, Cu, Zn).[11b] Accordingly, the observed 15-line spectrum can be attributed to the 2:1 mixture of the C_{2h}-symmetric anti isomer and the C_{2v}-symmetric syn isomer of **1**, each of which giving eight signals in a 2:2:2:1:2:2:2:2 intensity ratio. Thus, the more intense signals at −87 (relative intensity 4, J_{W-O-P} 1.4 Hz), −155 (4, J_{W-O-P} 0.8 Hz), −158 (2, J_{W-O-P} 1.5 Hz), −159.5 (4, J_{W-O-P} 1.8 Hz), −236 (4, J_{W-O-P} 1.9 Hz), −243 (4, J_{W-O-P} 1.75 Hz), −245.4 (4, J_{W-O-P} 1.65 Hz) belong to the anti isomer of **1**, while the weaker signals at −91 (2), −156 (2), −159 (1), −160.4 (2), −236.6 (2), −243.6 (2), and −244.6 (2) could be assigned to the syn derivative. The peak at −136 (6) is attributed to the overlapping signals from both *anti*-**1** and *syn*-**1** species.

On the basis of their lower relative intensity, the signals at −158 ppm (*anti*-**1**) and −159 ppm (*syn*-**1**) are attributed to the unique polar W^{VI} centers of the $\{P_2W_{15}\}$ ligands. The chemical shift values for these signals are in a good agreement with the literature data for $[\alpha\text{-}H_xP_2W_{15}Nb_3O_{62}]^{(9-x)-}$,[15] $[\alpha\text{-}H_3P_2W_{15}O_{59}\{Al(OH_2)\}_3]^{6-}$,[16] and $[\alpha\text{-}P_2W_{15}Ti_3O_{62}]^{12-}$ [17] polyanions with C_{3v} symmetry, for which the signals corresponding to the W^{VI} centers of the W_3O_6 caps appear at −148.0, −156.6, and −148.3 ppm, respectively, as well as with observation of signal at −150.4 ppm for the unique W^{VI} centers in $\{Zn_4(P_2W_{15})_2\}$.[11b] Unfortunately, very close spacing of the signals for the both isomers complicates their direct assignment

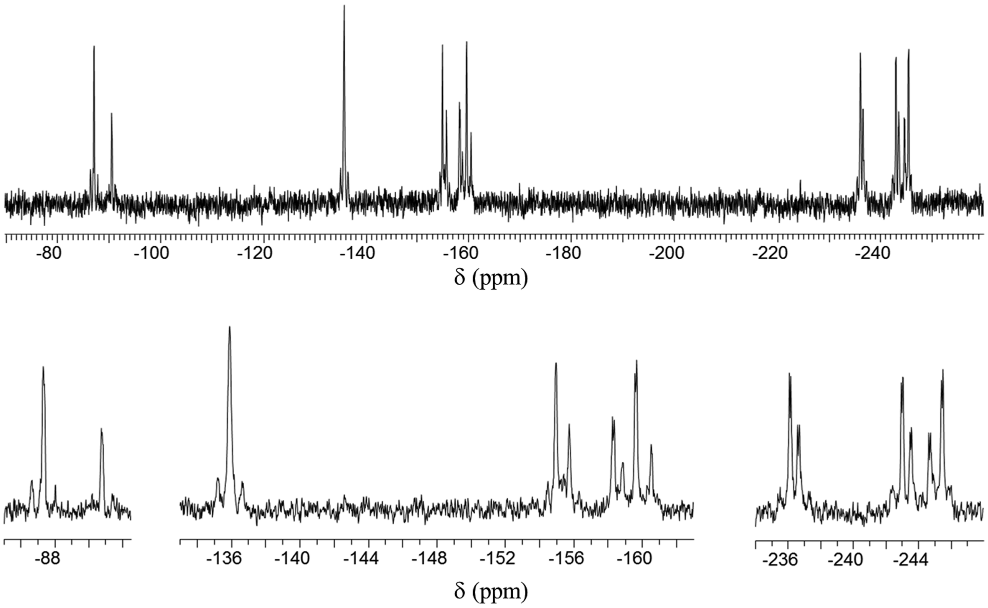

Figure 3. Room temperature ^{183}W NMR spectrum of **Na-1** redissolved in H_2O/D_2O after exponential multiplication with a line broadening of 0.5 Hz (top) and close-up of the signals (bottom).

based on J_{W-O-W} values; however, the attribution of the remaining signals can be based on the similarity to the ^{183}W NMR spectrum of the related $\{Zn_4(P_2W_{15})_2\}$[11b] complex (for which 2D INADEQUATE $^{183}W\{^{31}P\}$ NMR measurements allowed unambiguous attribution of all peaks) and logical reasoning. Thus, the three closely spaced upfield signals (at −236, −243, and −245.4 for *anti*-**1** and −236.6, −243.6 and −244.6 for *syn*-**1**) most likely belong to the W^{VI} centers of the inner W_6O_{27} belt of $\{P_2W_{15}\}$ (arranged around the P^AO_4 group like the W_3O_6 cap). This proposition is in a good agreement with observation of the signals for the inner W_6O_{27} belt of $\{P_2W_{15}\}$ units in $\{Zn_4(P_2W_{15})_2\}$ at −238.4, −243.4, and −244.7 ppm. The signal at −159.5 ppm shows the same splitting due to J_{P-O-W} coupling (~1.8 Hz) as that of the unique polar W^{VI} center. This suggests that the signals at −159.5 ppm (for *anti*-**1**) and −160.4 ppm (for *syn*-**1**) also belong to the W centers of the W_3O_{13} caps connected with the P^B atom through the O atom that is common to all the three tungstens. Then the remaining three signals that are shifted to significantly higher frequencies relative the spectrum range of $\{Zn_4(P_2W_{15})_2\}$ relate to the W atoms connected to palladium. It is also logical to suggest that the six W^{VI} centers close to the lacunary site of the $\{P_2W_{15}\}$ units in **1** are less shielded compared to the other W^{VI} centers due to the square-planar coordination environment of the Pd^{II} ions and subsequently give the three most downfield signals (at −87, −136, and −155 ppm for *anti*-**1** and −91, −136, and −156 ppm for *syn*-**1**). At that, the downfield shift of these signals in comparison with the corresponding signals in the ^{183}W NMR spectrum for $\{Zn_4(P_2W_{15})_2\}$[11b] is consistent with a weaker binding of the $\{P_2W_{15}\}$ ligands to the Pd^{II} centers in **1** than to the Zn^{II} centers in $\{Zn_4(P_2W_{15})_2\}$, which is in full agreement with the different coordination geometries of the Pd^{II} and Zn^{II} centers in these structures. We further hypothesize that the signal at −136 ppm may possibly correspond to the W^{VI} centers binding the oxygens coordinated by Pd^{II} centers of the first structural type, as such W^{VI} centers have very similar coordination environment in the both *anti*-**1** and *syn*-**1** derivatives.

UV−Vis Spectroscopy. The solutions of **Na-1** were further examined using absorption spectroscopy. The UV−vis spectrum of **Na-1** in 0.5 M CH_3COONa aqueous solution (pH = 4.3), shown in the Supporting Information (Figure S7), exhibits a strong absorption maximum at 236 nm (ε = 166 167 M^{-1} cm^{-1}) followed by a broad shoulder at about 292 nm (ε = 81 495 M^{-1} cm^{-1}) in the UV light area and a less intense absorption maximum at 477 nm (ε = 2374 M^{-1} cm^{-1}) in the visible light area. The spectrum remains unchanged for at least 1 week for both more (6.7×10^{-4} M) and less (4.7×10^{-5} M) concentrated solutions, confirming the stability of polyanions **1** in 0.5 M CH_3COONa aqueous medium at pH 4.3.

The spectra of **Na-1** solutions in 1 M CH_3COOH (pH 2.0) and 1 M CH_3COONa at various pH values are shown in the Supporting Information (Figure S10). The solutions were prepared independently by taking equal amounts of **Na-1** and equal amounts of the corresponding solvent. The obtained spectra showed the highest absorption at about 477 nm in the solutions with a pH range of 2−4, suggesting the highest stability of **1** in these media. The spectra at pH 2.0 and 4.0 remained unchanged for at least 1 day, while it was not possible to monitor the stability of **1** in the solutions with higher pH values due to the lower solubility and recrystallization of **Na-1**, which occurs within several hours.

■ CONCLUSIONS

In our investigation of the reactivity of Pd^{II} ions toward trilacunary derivative of Wells−Dawson-type phosphotungstates $[\alpha\text{-}P_2W_{15}O_{56}]^{12-}$ in 0.5 M CH_3COONa media, the tetranuclear sandwich-like complex $[Pd_4(\alpha\text{-}P_2W_{15}O_{56})_2]^{16-}$ was found to self-assemble in a wide range of pH, Pd^{II}:$\{P_2W_{15}\}$ ratios, and reaction temperatures. The $[Pd_4(\alpha\text{-}P_2W_{15}O_{56})_2]^{16-}$ clusters exist as syn and anti isomers that vary in the relative orientation of the two $\{P_2W_{15}\}$ ligands and form in a 2:1 ratio. Due to square-planar Pd^{II} coordination, the title structure differs from conventional (transition metal-substituted) $\{M_4(P_2W_{15})_2\}$ species, despite the similar rhombic arrangement of the four heterometal ions in these complexes. The arrangement of Pd^{II} centers in **1** also differs markedly from Pd^{II} complexes with trilacunary Keggin-type polyoxotungstates, because of the slightly different structure of the vacant sites in these POTs. ^{31}P and ^{183}W NMR spectroscopy demonstrated the long-term solution stability of polyanions **1** in aqueous media.

■ EXPERIMENTAL SECTION

General Methods and Materials. The reagents were used as purchased without further purification. $Na_{12}[\alpha\text{-}P_2W_{15}O_{56}]\cdot 24H_2O$ was obtained according to the reported procedure[11a,12] starting from $K_6[\alpha\text{-}P_2W_{18}O_{62}]\cdot 14H_2O$.[12,13] Elemental analysis results (ICP-OES, C/H/N) were obtained from Central Institute for Engineering, Electronics

Table 1. Crystal Data and Structure Refinement for Na-1

empirical formula	$H_{142}Na_{16}O_{183}P_4Pd_4W_{30}$
formula weight, g/mol	9503.96
crystal system	triclinic
space group	$P\bar{1}$
a, Å	14.0333(3)
b, Å	14.0985(3)
c, Å	25.2703(5)
α, deg	83.9425(17)
β, deg	76.5160(19)
γ, deg	60.514(2)
volume, $Å^3$	4231.88(16)
Z	1
D_{calc}, g/cm^3	3.729
absorption coeff, mm^{-1}	20.912
$F(000)$	4246
crystal size, mm	0.06 × 0.06 × 0.13
θ range for data collection, deg	4.09−25.03
completeness to Θ_{max}	98.5%
index ranges	$-16 \le h \le 16$ $-16 \le k \le 16$ $-30 \le l \le 30$
reflections collected	75 309
independent reflections	14 717
R_{int}	0.0722
observed ($I > 2\sigma(I)$)	13 246
absorption correction	empirical using spherical harmonics
T_{min}/T_{max}	0.0822/0.3732
data/restraints/parameters	14 717/24/663
goodness-of-fit on F^2	1.109
R_1, wR_2 ($I > 2\sigma(I)$)	R_1 = 0.0722, wR_2 = 0.1829
R_1, wR_2 (all data)	R_1 = 0.0781, wR_2 = 0.1874
largest diff peak and hole, e $Å^{-3}$	3.876 and −3.061

and Analytics (ZEA-3), Forschungszentrum Jülich GmbH (Jülich, Germany). Vibrational spectra were recorded on a Bruker VERTEX 70 FT-IR spectrometer coupled with a RAM II FT-Raman module (1064 nm Nd:YAG laser) on KBr disks for the FT-IR and the solid material for the Raman measurements. UV−vis spectra were measured using 10 mm quartz cuvettes on an Analytik Jena Specord S600 spectrophotometer. ^{31}P NMR spectra were recorded at room temperature in 5 mm tubes using a Bruker Avance 600-MHz spectrometer equipped with a prodigy probe, operating at 242.95 MHz for ^{31}P, and with a Varian Inova 400 MHz spectrometer equipped with an Auto-X-PFG-probe with a resonance frequency of 161.834 MHz. Chemical shifts are reported with respect to 85% H_3PO_4; all chemical shifts downfield of the reference are reported as positive values. ^{183}W NMR spectra of **Na-1** solution in H_2O/D_2O ($c \sim 1 \times 10^{-2}$ M) were recorded in 10 mm tubes on a Bruker Avance 400 MHz instrument at room temperature with a resonance frequency of 16.67 MHz. The chemical shifts are reported with respect to 1 M Na_2WO_4 aqueous solution as a reference.

Synthesis of $Na_{16}[Pd_4(\alpha\text{-}P_2W_{15}O_{56})_2]\cdot 71H_2O$ (Na-1). A sample of $Na_{12}[\alpha\text{-}P_2W_{15}O_{56}]\cdot 24H_2O$ (0.450 g, 0.102 mmol) was dissolved in 9 mL of 0.5 M CH_3COONa buffer (pH 4.2) under vigorous stirring. Solid $Pd(NO_3)_2\cdot 2H_2O$ (0.075 g, 0.281 mmol) was added to the obtained solution and the reaction mixture was stirred for another 60 min at room temperature and then filtered and left for evaporation at room temperature, being divided into two or three vials. Brown crystals of **Na-1** (rhombic plates) form within 1−2 weeks. The crystals were collected by filtration, washed with ice-cold water, and dried in air. Yield: 0.27 g (55% based on $\{P_2W_{15}\}$). Anal. Calcd for $H_{142}Na_{16}O_{183}P_4Pd_4W_{30}$ (found): Na, 3.87 (3.86); P, 1.30 (1.32); Pd, 4.48 (4.48); W, 58.03 (58.0). IR spectrum (KBr pellet), cm^{-1}: 3434 (s, br), 1621 (s), 1090 (s), 1065 (m), 1016 (m), 941 (s), 909 (s), 831 (s), 767 (s), 598 (m), 563 (m), 527 (m), 394 (w), 376 (w). Raman (in solid), cm^{-1}: 984 (s), 964 (s), 887 (m), 822 (w), 526 (w), 374 (w), 324 (w), 226 (w), 164 (w), 118 (w). ^{31}P NMR (H_2O/D_2O) *anti*-**1**, δ: −3.4, −14.6 ppm. ^{31}P NMR (H_2O/D_2O) *syn*-**1**, δ: −3.6, −14.6 ppm. ^{183}W NMR (H_2O/D_2O) *anti*-**1**, δ: −87 (2 W), −136 (2 W), −155 (2 W), −158 (1 W), −159.5 (2 W), −236 (2 W), −243 (2 W), −245.4 (2 W) ppm. ^{183}W NMR (H_2O/D_2O) *syn*-**1**, δ: −91 (2 W), −136 (2 W), −156 (2 W), −159 (1 W), −160.4 (2 W), −236.6 (2 W), −243.6 (2 W), −244.6 (2 W) ppm. UV−vis (0.5 M CH_3COONa buffer solution, pH 4.3): λ = 236 nm, ε = 166 167 M^{-1} cm^{-1}; λ = 292 nm, ε = 81 495 M^{-1} cm^{-1}; λ = 477 nm, ε = 2374 M^{-1} cm^{-1}.

Synthesis of $[(C_4H_9)_4N]_{15}[HPd_4(\alpha\text{-}P_2W_{15}O_{56})_2]$ (TBA-1). A solution of **Na-1** (0.100 g, 0.010 mmol) in 3 mL of H_2O was dropwise added to an aqueous solution of $[(C_4H_9)_4N]HSO_4$ (0.080 g, 0.236 mmol, 2 mL of H_2O) under vigorous stirring. The mixture was acidified with 1 drop of 2 M HNO_3. The obtained precipitate of **TBA-1** was filtered on a glass frit, washed with plenty of water, and dried in air. Anal. Calcd for $C_{240}H_{541}N_{15}O_{112}P_4Pd_4W_{30}$ (found): C, 25.08 (24.04); H, 4.74 (4.77); N, 1.83 (1.90). IR spectrum (KBr pellet), cm^{-1}: 3468 (m, br), 2961 (s), 2934 (m), 2873 (m), 630 (w), 1484 (m), 1383 (m), 1237 (w), 1167 (m), 1094 (s), 1064 (m), 1025 (w), 999 (w), 958 (s), 902 (s), 779 (s, br), 597 (m), 595 (m), 560 (m), 530 (m), 430 (w), 392 (m).

X-ray Crystallography. Single-crystal diffraction data for **Na-1** were collected on a SuperNova (Agilent Technologies) diffractometer with Mo Kα radiation (λ = 0.710 73 Å) at 120 K. A crystal was mounted in a Hampton cryoloop with Paratone-N oil to prevent water loss. Absorption corrections were applied numerically on the basis of a multifaceted crystal model using CrysAlis software.[18] The SHELXTL software package[19] was used to solve and refine the structure. The structure was solved by direct methods and refined by full-matrix least-squares method against $|F|^2$ with anisotropic thermal parameters for all heavy POM skeleton atoms (Pd, P, W) and sodium countercations. The hydrogen atoms of the crystal waters were not located. The relative site occupancy factors for the disordered positions of tungsten, palladium, and oxygen atoms due to the $\{Pd_4P_2W_{15}\}/\{P_2W_{15}\}$ ligands rotation by 60° were refined using the PART instruction combined with EADP restrictions for the heavy atoms and then fixed at the obtained values and refined normally. The relative site occupancy factors for the disordered solvent oxygens were first refined in an isotropic approximation with U_{iso} = 0.05 and then fixed at the obtained values and refined without the thermal parameters restrictions.

The number of crystal water molecules and sodium countercations found by XRD was smaller than that determined by elemental analysis (32 vs 71 for H_2O and 7 vs 16 for Na^+, respectively) which could be explained by the high degree of disorder in the solid-state structure of **Na-1**. This is also consistent with large solvent-accessible volume remained in the structure. For overall consistency, the formula shown in the CIF file corresponds to the bulk material and has the same number of countercations and crystallization water molecules as found by elemental analysis, since all further studies are/will be performed on the isolated bulk material of **Na-1**.

Additional crystallographic data are summarized in Table 1. Further details on the crystal structure investigation may be obtained from Fachinformationszentrum Karlsruhe, 76344 Eggenstein-Leopoldshafen, Germany [fax (+49) 7247-808-666; e-mail crysdata@fiz-karlsruhe.de], upon quoting the depository number CSD 428389.

■ ASSOCIATED CONTENT

Ⓢ Supporting Information

Crystallographic data in CIF format; IR, NMR, and UV−vis−NIR spectra; and structure of $\{P_2W_{15}\}$ and its vacant site and comparison of the $\{Pd_4(P_2W_{15})_2\}$ structure with the structures of $\{M_4(P_2W_{15})_2\}$ and $\{Pd_3(XW_9)_2\}$ polyanions. This material is available free of charge via the Internet at http://pubs.acs.org.

■ AUTHOR INFORMATION

Corresponding Author

*E-mail: paul.koegerler@ac.rwth-aachen.de.

Author Contributions

The manuscript was written through contributions of all authors. All authors have given approval to the final version of the manuscript.

Notes

The authors declare no competing financial interest.

$^{\perp}$On leave from Nikolaev Institute of Inorganic Chemistry, 630090 Novosibirsk, Russia.

■ ACKNOWLEDGMENTS

Financial support was provided to P.K. by the European Commission (ERC Starting Grant MOLSPINTRON, no. 308051).

■ REFERENCES

(1) (a) Neumann, R.; Khenkin, A. M. *Inorg. Chem.* **1995**, *34*, 5753−5760. (b) Kuznetsova, N. I.; Detusheva, L. G.; Kuznetsova, L. I.; Fedotov, M. A.; Likholobov, V. A. *J. Mol. Catal. A: Chem.* **1996**, *114*, 131−139. (c) Gazarov, R. A.; Shirokov, V. A.; Petrov, P. A.; Dyatlov, V. A.; Egorov, Yu. A. Patent of Russian Federation No. 2064828, 1996. (d) Neumann, R.; Khenkin, A. M.; Juwiler, D.; Miller, H.; Gara, M. *J. Mol. Catal.A Chem.* **1997**, *117*, 169−183. (e) Vorontsova, I. V.; Korovchenko, P. A.; Gazarov, R. A. *Mendeleev Chem. J.* **1998**, *42*, 242−247. (f) Xie, Y.; Sun, W. L.; Liu, H. Z.; Kong, J. L.; Xie, G. Y.; Deng, J. Q. *Chem. Res. Chin. Univ.* **1998**, *14*, 87−89. (g) Xie, Y.; Sun, W. L.; Liu, H. Z.; Kong, J. L.; Xie, G. Y.; Deng, J. Q. *Anal. Lett.* **1998**, *31*, 2009−2024. (h) Duan, D.-L.; Wang, Z.-Z.; Gu, Y.-W.; Yang, A.-M. *Yunnan Daxue Xuebao, Ziran Kexueban* **2001**, *23*, 447−453. (i) Kogan, V.; Aizenshtat, Z.; Neumann, R. *New J. Chem.* **2002**, *26*, 272−274. (j) Adam, W.; Alsters, P. L.; Neumann, R.; Saha-Möller, C. R.; Sloboda-Rozner, S.; Zhang, R. *J. Org. Chem.* **2003**, *68*, 1721−1728. (k) Adam, W.; Alsters, P. L.; Neumann, R.; Saha-Möller, C. R.; Seebach, D.; Beck, A.; Zhang, R. *J. Org. Chem.* **2003**, *68*, 8222−8231. (l) Stapleton, A. J.; Sloan, M. E.; Napper, N. J.; Burns, R. C. *Dalton Trans.* **2009**, 9603−9615. (m) Hirano, T.; Uehara, K.; Kamata, K.; Mizuno, N. *J. Am. Chem. Soc.* **2012**, *134*, 6425−6433. (n) Tong, J. H.; Wang, H. Y.; Cai, X. D.; Zhang, Q. P.; Ma, H. C.; Lei, Z. Q. *Appl.*

Organomet. Chem. **2014**, *28*, 95−100. (o) Villanneau, R.; Roucoux, A.; Beaunier, P.; Brourief, D.; Proust, A. *RSC Adv.* **2014**, *4*, 26491−26498.

(2) (a) Putaj, P.; Lefebvre, F. *Coord. Chem. Rev.* **2011**, *255*, 1642−1685. (b) Izarova, N. V.; Pope, M. T.; Kortz, U. *Angew. Chem., Int. Ed.* **2012**, *51*, 9492−9510.

(3) (a) Chubarova, E. V.; Dickman, M. H.; Keita, B.; Nadjo, L.; Miserque, F.; Mifsud, M.; Arends, I. W. C. E.; Kortz, U. *Angew. Chem., Int. Ed.* **2008**, *47*, 9542. (b) Izarova, N. V.; Vankova, N.; Heine, T.; Ngo Biboum, R.; Keita, B.; Nadjo, L.; Kortz, U. *Angew. Chem., Int. Ed.* **2010**, *49*, 1886−1889. (c) Izarova, N. V.; Kondinski, A.; Vankova, N.; Heine, T.; Jäger, P.; Schinle, F.; Hampe, O.; Kortz, U. *Chem.—Eur. J.* **2014**, *20*, 8556−8560.

(4) Cameron, J. M.; Gao, J.; Long, D.-L.; Cronin, L. *Inorg. Chem. Front.* **2014**, *1*, 178−185.

(5) (a) Angus-Dunne, S. J.; Burns, R. C.; Craig, D. C.; Lawrance, G. A. *J. Chem. Soc., Chem. Commun.* **1994**, 523−524. (b) Maksimov, G. M.; Maksimovskaya, R. I.; Matveev, K. I. *Russ. J. Inorg. Chem.* **1987**, *32*, 551−555. (c) Izarova, N. V.; Banerjee, A.; Kortz, U. *Inorg. Chem.* **2011**, *50*, 10379−10386.

(6) Hirano, T.; Uehara, K.; Uchida, S.; Hibino, M.; Kamata, K.; Mizuno, N. *Inorg. Chem.* **2013**, *52*, 2662−2670.

(7) (a) Knoth, W. H.; Domaille, P. J.; Harlow, R. L. *Inorg. Chem.* **1986**, *25*, 1577−1584. (b) Detusheva, L. G.; Kuznetsova, L. I.; Fedotov, M. A.; Likholobov, V. A.; Dovlitova, L. S.; Vlasov, A. A.; Malakhov, V. V. *Russ. J. Coord. Chem.* **2001**, *27*, 838−845. (c) Villanneau, R.; Renaudineau, S.; Herson, P.; Boubekeur, K.; Thouvenot, R.; Proust, A. *Eur. J. Inorg. Chem.* **2009**, 479−488. (d) Bi, L.-H.; Kortz, U.; Keita, B.; Nadjo, L.; Borrmann, H. *Inorg. Chem.* **2004**, *43*, 8367−8372.

(8) (a) Krebs, B.; Droste, E.; Piepenbrink, M. In *Polyoxometalate Chemistry. From Topology via Self-Assembly to Applications*; Pope, M. T., Müller, A., Eds.; Kluwer: Dordrecht, 2001; pp 89−99. (b) Bi, L.-H.; Reicke, M.; Kortz, U.; Keita, B.; Nadjo, L.; Clark, R. J. *Inorg. Chem.* **2004**, *43*, 3915−3920. (c) Bi, L.-H.; Kortz, U.; Keita, B.; Nadjo, L.; Daniels, L. *Eur. J. Inorg. Chem.* **2005**, 3034−3041. (d) Gao, J.; Yan, J.; Beeg, S.; Long, D.-L.; Cronin, L. *Angew. Chem., Int. Ed.* **2012**, *51*, 3373−3376.

(9) Bi, L.-H.; Dickman, M. H.; Kortz, U. *CrystEngComm* **2009**, *11*, 965−966.

(10) Sokolov, M. N.; Kalinina, I. V.; Peresypkina, E. V.; Moroz, N. K.; Naumov, D. Y.; Fedin, V. P. *Eur. J. Inorg. Chem.* **2013**, 1772−1779.

(11) See, for example, the following: (a) Finke, R. G.; Droege, M. W. *Inorg. Chem.* **1983**, *22*, 1006−1008. (b) Finke, R. G.; Droege, M. W.; Domaille, P. J. *Inorg. Chem.* **1987**, *26*, 3886−3896. (c) Weakley, T. J. R.; Finke, R. G. *Inorg. Chem.* **1990**, *29*, 1235−1241. (d) Finke, R. G.; Weakley, T. J. R. *J. Chem. Crystallogr.* **1994**, *24*, 123−128. (e) Gómez-García, C. J.; Borrás-Almenar, J. J.; Coronado, E.; Ouahab, L. *Inorg. Chem.* **1994**, *33*, 4016−4022. (f) Kirby, J. F.; Baker, L. C. W. *J. Am. Chem. Soc.* **1995**, *117*, 10010−10016. (g) Zhang, X.; Chen, Q.; Duncan, D. C.; Campana, C.; Hill, C. L. *Inorg. Chem.* **1997**, *36*, 4208−4215. (h) Anderson, T. M.; Zhang, X.; Hardcastle, K. I.; Hill, C. L. *Inorg. Chem.* **2002**, *41*, 2477−2488. (i) Ruhlmann, L.; Nadjo, L.; Canny, J.; Thouvenot, R. *Eur. J. Inorg. Chem.* **2002**, 975−986. (j) Mbomekalle, I. M.; Keita, B.; Nadjo, L.; Berthet, P.; Hardcastle, K. I.; Hill, C. L.; Anderson, T. M. *Inorg. Chem.* **2003**, *42*, 1163−1169. (k) Mbomekalle, I. M.; Keita, B.; Nadjo, L.; Berthet, P.; Neiwert, W. A.; Hill, C. L.; Ritorto, M. D.; Anderson, T. M. *Dalton Trans.* **2003**, 2646−2650. (l) Ruhlmann, L.; Schaming, D.; Ahmed, I.; Courville, A.; Canny, J.; Thouvenot, R. *Inorg. Chem.* **2012**, *51*, 8202−8211. (m) Yao, S.; Yan, J.; Yu, Y.; Wang, E.-B. *J. Coord. Chem.* **2012**, *65*, 1451−1458.

(12) Contant, R. *Inorg. Synth.* **1990**, *27*, 104−111.

(13) Wu, H. *J. Biol. Chem.* **1920**, *43*, 189−220.

(14) (a) Parker, S. F.; Refson, K.; Hannon, A. C.; Barney, E. R.; Robertson, S. J.; Albers, P. *J. Phys. Chem. C* **2010**, *114*, 14164−14172. (b) Barsukova, M.; Izarova, N. V.; Ngo Biboum, R.; Keita, B.; Nadjo, L.; Ramachandran, V.; Dalal, N. S.; Antonova, N. S.; Carbó, J. J.; Poblet, J. M.; Kortz, U. *Chem.—Eur. J.* **2010**, *16*, 9076−9085.

(15) Edlund, D. J.; Saxton, R. J.; Lyon, D. K.; Finke, R. G. *Organometallics* **1988**, *7*, 1692−1704.

(16) Kato, C. N.; Kashiwagi, T.; Unno, W.; Nakagawa, M.; Uno, H. *Inorg. Chem.* **2014**, *53*, 4824−4832.

(17) Meng, L.; Liu, J. F. *Transition Met. Chem.* **1995**, *20*, 188−190.

(18) CrysAlisPro, Version 1.171.36.21 (release 14−08−2012 CrysAlis171.NET), Agilent Technologies, Santa Barbara, CA.

(19) Sheldrick, G. M. *Acta Crystallogr.* **2008**, *A64*, 112−122.